EXIT-Chart Optimized Short Block Codes for Iterative Joint Source and Channel Decoding in H.264 Video Telephony

Nasruminallah and Lajos Hanzo, *Fellow, IEEE*

***Abstract*—In this paper, we propose a family of short block codes (SBCs) designed for guaranteed convergence in soft-bit-assisted iterative joint source and channel decoding, which facilitate improved iterative soft-bit source decoding (SBSD) and channel decoding. Data-partitioned (DP) H.264 source-coded video is used to evaluate the performance of our system using SBC-assisted SBSD, in conjunction with recursive systematic convolution (RSC) codes for transmission over correlated narrow-band Rayleigh fading channels. The effect of different SBC schemes having diverse minimum Hamming distances $d_{\mathrm{H,min}}$ and code rates on the attainable system performance is demonstrated, when using iterative SBSD and channel decoding, while keeping the overall bit rate budget constant by appropriately partitioning the total available bit rate budget between the source and channel codecs to improve the overall bit error rate (BER) performance and to enhance the objective video quality expressed in terms of peak signal-to-noise ratio (PSNR).[1] EXtrinsic Information Transfer (EXIT) charts were used to analyze the attainable system performance. Explicitly, our experimental results show that the proposed error protection scheme using rate-1/3 SBCs having $d_{\mathrm{H,min}} = 6$ outperforms the identical-rate SBCs having $d_{\mathrm{H,min}} = 3$ by about 2.25 dB at the PSNR degradation point of 1 dB. Additionally, an E_b/N_0 gain of 9 dB was achieved, compared with the rate-5/6 SBC having $d_{\mathrm{H,min}} = 2$ and an identical overall code rate. Furthermore, an E_b/N_0 gain of 25 dB is attained at the PSNR degradation point of 1 dB while using iterative soft-bit source and channel decoding with the aid of rate-1/3 SBCs relative to the identical-rate benchmarker.**

***Index Terms*—EXtrinsic Information Transfer (EXIT) charts, H.264/AVC, iterative source-channel decoding (ISCD), peak signal-to-noise ratio (PSNR), recursive systematic convolutional (RSC) codes, short block codes (SBCs), soft-bit source decoding (SBSD), wireless video transmission.**

I. Motivation and Background

RELIABLE transmission of multimedia source-coded streams over diverse wireless communication networks constitutes a challenging research topic [1], [2]. Since the early days of wireless video communications [3]–[6], substantial further advances have been made in the field of both proprietary and standard-based solutions [7], [8]. Furthermore, the joint optimization of different functions such as joint source and channel decoding (JSCD) has gained considerable attention. The family of JSCD schemes often relies on exploiting the residual redundancy in the source-coded bit stream. Fingscheidt and Vary [9] and Fingscheidt *et al.* [10] proposed soft-bit source decoding (SBSD) to exploit the natural residual redundancy of the source-coded bit stream for improving the convergence of iterative source-channel decoding (ISCD) [11], [12]. However, only moderate residual redundancy is left in the source-coded bit stream when using advanced state-of-the-art coding techniques. Therefore, we propose to deliberately impose additional redundancy on the source-coded bit stream with the aid of the novel class of SBCs proposed. In our experimental setup, the H.264/AVC video codec [13] is used to encode the input video sequence and generate the source-coded bit stream. The H.264/AVC codec employs heterogeneous variable length coding and predictive coding techniques to achieve high compression efficiency, which makes the compressed bit stream susceptible to transmission errors [1]. A single bit error in the coded stream may corrupt the decoding of numerous future codewords. Moreover, due to predictive coding, the effects of channel errors may affect the neighboring video blocks due to error propagation. Therefore, the transmission of compressed video over wireless systems is a challenging task. Various error-resilient schemes have been proposed in [1] to alleviate these problems, but the price paid is potential reduction in the achievable compression efficiency and increase in computational complexity. An iterative joint source-channel decoding procedure inspired by the concept of serial concatenated codes was presented in [14]. A symbol-based soft-input *a posteriori* probability decoder was presented in [15], where the residual redundancy was exploited for improved error protection. Instead of the traditional serial concatenation of the classic variable length codes (VLCs) with a channel code, a parallel concatenated coding scheme was presented in [16], where the VLCs were combined with a turbo code. On the other hand, a novel irregular variable length coding (IrVLC) scheme designed for near-capacity joint source and channel coding was proposed in [17]. Likewise, Hanzo *et al.* [7] advocated the employment of state-of-the-art high-speed-packet-access-style [18] burst-by-burst adaptive transceivers for interactive cellular and cordless video telephony, which are capable of accommodating

Manuscript received August 10, 2008; revised January 5, 2009, March 10, 2009, and March 23, 2009. First published April 7, 2009; current version published October 2, 2009. The review of this paper was coordinated by Prof. H. Nguyen.

The authors are with the School of Electronics and Computer Science, University of Southampton, SO17 1BJ Southampton, U.K. (e-mail: lh@ecs.soton.ac.uk; n06r@ecs.soton.ac.uk).

Digital Object Identifier 10.1109/TVT.2009.2020578

[1]PSNR is the most widely used and simplest form of objective video quality measure that represents the ratio of the peak-to-peak signal to the root-mean-squared noise [1].

time-variant channel quality fluctuation of wireless channels. An iterative-source-and-channel-decoding-aided irregular convolutional coded videophone scheme using reversible variable-length codes and the maximum *a posteriori* (MAP) [19] detection algorithm was proposed in [20]. The performance analysis of soft-bit-assisted iterative JSCD was presented in [21], where differential-space-time-spreading-aided sphere-packing modulation was invoked, which dispensed with channel estimation and provided both spatio-temporal diversity and multiuser support. Furthermore, a joint source-channel decoding method based on the MAP algorithm was proposed by Wang and Yu [22]. Instead of the well-known convolutional coded ISCD, an ISCD based on two serial concatenated short block codes (SBCs) was proposed by Clevorn *et al.* [23]. In the aforementioned scheme, a (6, 3) outer block code served as a redundant index assignment, whereas a rate-1 block code was used as inner code. Similarly, Thobaben [24] provided the performance analysis of a single-parity check code with rate $R = 4/5$ used to protect the quantized source symbols relative to specifically designed VLCs. Joint source channel coding schemes employing a linear block code with rate $R = 4/5$ to map the quantized source symbols to a binary representation were combined with an inner irregular channel encoder in [25]. An optimized bit rate allocation scheme using an inner channel encoder with rate $r^\star = 1$,[2] along with $k = 3$ to $k^\star = 6$ source mapping, was proposed in [26], and its performance was evaluated relative to conventional ISCD using a recursive nonsystematic convolutional inner code with rate $r = 1/2$. The turbo decodulation scheme presented in [27] and [28] consisted of two iterative loops: The inner loop was composed of the two components of bit-interleaved coded modulation using iterative decoding, and the outer loop was constituted by the ISCD scheme. By contrast, in [29], SBC-based redundant index assignment and multidimensional mapping were used to artificially introduce redundancy, and a single iterative loop was employed. Similarly, Clevorn *et al.* [30] presented new design and optimization guidelines for performance improvement of the ISCD using the concept of redundant index assignment with specific generator matrices.

In contrast to this background, where specific mapping examples were provided for iterative source and channel coding, we present powerful yet low-complexity algorithms for SBCs, which can be used to generate SBCs for a variety of mapping rates associated with diverse $d_{\mathrm{H,min}}$ values that are applicable to wide-ranging multimedia services. Additionally, instead of modeling the sources with the aid of their correlation, the practically achievable interactive video performance trends are quantified when using state-of-the-art video-coding techniques, such as H.264/AVC. More explicitly, instead of assuming a specific source-correlation model, we based our system design examples on the simulation of the actual H.264/AVC source-coded bit stream. The SBC-aided SBSD scheme was utilized for protecting the H.264-coded bit stream using recursive systematic convolution (RSC) codes [19]. The SBC coding scheme was incorporated by carefully partitioning the total available bit rate budget between the source and channel codecs, which results in an improved performance when ISCD is employed. Explicitly, an E_b/N_0 gain of 25 dB is attained using ISCD, when employing a rate-1/3 SBC scheme, in comparison with a realistic identical-rate benchmarker dispensing with the SBC scheme.

The rest of this paper is organized as follows: In Section II, we portray our system model, along with an overview of the H.264 encoded bit stream and SBSD. An overview of ISCD is provided in Section III, along with our proposed SBC coding algorithms, accompanied by a design example. Section IV provides the EXtrinsic Information Transfer (EXIT) chart analysis of our proposed system model, whereas the performance of the proposed system is characterized with the aid of our simulation results in Section V. Finally, we offer our conclusions in Section VI.

II. System Overview

A. H.264-Coded Stream Structure

The H.264/AVC codec's structure is notionally divided into the video-coding layer (VCL) and the network abstraction layer (NAL) [31]. The hybrid video-coding functions designed for improved coding efficiency are part of the VCL, whereas the NAL is designed for improved network adaptation and is responsible for the reliable transport of the resultant bit stream generated by the VCL over a wide range of transport layer protocols. The H.264/AVC generates a number of video-frame slices, which are formed by an integer number of consecutive macro blocks (MBs) of a picture. The number of MBs per slice may vary from a single MB to all the MBs of a picture in a given slice. Error-resilient data partitioning (DP) [32] has been incorporated in the H.264/AVC codec to mitigate the effects of channel errors. In the H.264/AVC codec, DP results in three different types of streams per slice, which are referred to as Type-A, -B, and -C partitions, each containing specific sets of coding parameters having different levels of importance. Additionally, the H.264-coded stream contains information related to the group-of-pictures sequence and a so-called picture parameter set containing information related to all the slices of a single picture. All these different syntax elements are contained in NAL units (NALUs), which consist of a 1-B header and a payload of a variable number of bytes containing the coded symbols of the corresponding H.264 syntax element. The type of data contained by the NALU is identified by the 5-bit NALU type field contained in the NALU header.

B. System Model

The schematic of our proposed videophone arrangement used as our design example for quantifying the performance of various SBC schemes is shown in Fig. 1. At the transmitter side, the video sequence is compressed using the H.264 video codec, and video source bit stream x_k is mapped or encoded into bit string x'_m using the specific SBC coding scheme employed. Subsequently, the output bit string after SBC coding is interleaved using the bit interleaver Π of Fig. 1, yielding the interleaved sequence $\bar{x}_m$, which is then encoded by an RSC code having a specific code rate given in Table I. Interleaving and

[2]Superscript $\star$ was adopted from [26].

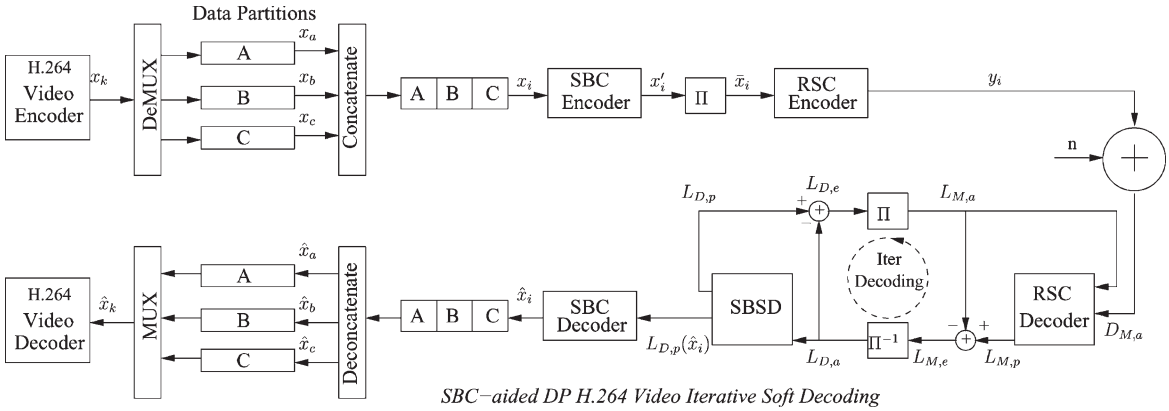

Fig. 1. Proposed system model.

TABLE I
DIFFERENT SBCs WITH CORRESPONDING SYMBOLS, MINIMUM HAMMING DISTANCES $d_{\mathrm{H,min}}$, AND CODE RATES

SBC Type		Symbols in Decimal	$d_{H,min}$	Code Rate		
	Rate-1 SBC	{0,1}	1	RSC 1/4	SBC 1	Overall 1/4
Algorithm-I	Rate-$\frac{2}{3}$ SBC$_{[2,\ 3]}$	{0,3,5,6}	2	3/8	2/3	1/4
	Rate-$\frac{3}{4}$ SBC$_{[3,\ 4]}$	{0,3,5,6,9,10,12,15}	2	1/3	3/4	1/4
	Rate-$\frac{4}{5}$ SBC$_{[4,\ 5]}$	{0,3,5,6,9,10,12,15,17,18,20,23,24,27,29,30}	2	5/16	4/5	1/4
	Rate-$\frac{5}{6}$ SBC$_{[5,\ 6]}$	{0,3,5,6,9,10,12,15,17,18,20,23,24,27,29,30,33, 34,36,39,40,43,45,46,48,51,53,54,57,58,60,63}	2	3/10	5/6	1/4
Algorithm-II	Rate-$\frac{1}{3}$ SBC$_{[2,\ 6]}$	{0,22,41,63}	3	3/4	1/3	1/4
	Rate-$\frac{1}{3}$ SBC$_{[3,\ 9]}$	{0,78,149,219,291,365,438,504}	4	3/4	1/3	1/4
	Rate-$\frac{1}{3}$ SBC$_{[4,\ 12]}$	{0,286,557,819,1099,1365,1638,1912,2183,2457, 2730,2996,3276,3538,3809,4095}	5	3/4	1/3	1/4
	Rate-$\frac{1}{3}$ SBC$_{[5,\ 15]}$	{0,1086,2141,3171,4251,5285,6342,7416,8471,9513, 10570,11636,12684,13746,14801,15855,16911,17969, 19026,20076,21140,22186,23241,24311,25368,26406, 27461,28539,29571,30653,31710,32736}	6	3/4	1/3	1/4
Algorithm-I	Rate-1 SBC	{0,1}	1	1/2	1	1/2
	Rate-$\frac{2}{3}$ SBC$_{[2,\ 3]}$	{0,3,5,6}	2	3/4	2/3	1/2

deinterleaving constitute an important step in the iterative decoder of Fig. 1, ensuring that the bits are input in their expected original order to the component decoders and ascertaining that the statistical independence of the extrinsic log-likelihood ratios (LLRs) is retained. Since, in addition to the specific design of the interleaver, the degree of statistical independence guaranteed by an interleaver is also related to its length [33], instead of independently performing the ISCD operation on the various frame slices, we concatenated all the bits generated by each type of partition for the different MBs within each slice of a given frame, which results in a longer interleaver without extending the video delay and hence improves the achievable performance of iterative decoding. The resultant bit stream is quaternary phase shift keying (QPSK) modulated and transmitted over a temporally correlated narrow-band Rayleigh fading channel associated with the normalized Doppler frequency of $f_d = f_D T_s = 0.01$, where f_D is the Doppler frequency, and T_s is the symbol duration. At the receiver, the signal is QPSK demodulated, and the resultant soft information is passed to the RSC decoder. The extracted extrinsic information is then exchanged between the SBSD and RSC decoders of Fig. 1 [11]. Following QPSK demodulation at the receiver, the soft information is extracted in the form of its LLR representation $D_{M,a}$. This soft information $D_{M,a}$ is forwarded to the RSC inner decoder, which processes it, along with the *a priori* information $L_{M,a}$ fed back from the outer decoder of Fig. 1, to generate the *a posteriori* LLR values $L_{M,p}$. The *a priori* LLR values $L_{M,a}$ fed back from the outer decoder are subtracted from the inner decoder's output *a posteriori* LLR values $L_{M,p}$ to generate the extrinsic LLR values $L_{M,e}$, which are subsequently deinterleaved by the soft-bit interleaver of Fig. 1, yielding the soft bits $L_{D,a}$ that is input to the outer decoder to compute the *a posteriori* LLR value $L_{D,p}$. Observe in Fig. 1 that $L_{D,e}$ is generated by subtracting the *a priori* information $L_{D,a}$ from the *a posteriori* information $L_{D,p}$, which, in turn, results in $L_{M,a}$ after interleaving. During iterative decoding, the outer decoder exploits the input LLR values for the sake of providing improved *a priori* information for the inner channel decoder of Fig. 1, which, in turn, exploits the fed-back *a priori* information in the subsequent iteration for the sake of providing improved *a posteriori* LLR values for the outer decoder. Further details about iterative decoding are provided in [34].

C. Soft-Bit Source Decoding

The conventional SBSD scheme gleans its extrinsic information from the natural residual redundancy, which inherently remains in the bit stream after source encoding and manifests itself in terms of the nonuniform probability of occurrence of the resultant bit patterns. More explicitly, for SBC coding, the source-encoded bit stream is partitioned into $M = 2^K$-ary or K-bit symbols, each of which has a different probability of occurrence and will be termed as the information word encoded by the proposed SBC. The redundancy of the source bit stream is then characterized with the aid of the nonuniform $M = 2^K$-ary symbol probability distribution $P[S_K(\tau)]$, where $S_K(\tau) = [S_K(1), S_K(2), \ldots, S_K(M)]$, with K denoting the number of bits in each $M = 2^K$-ary symbol.[3] Details regarding the extrinsic information generation algorithm using SBSD for the zero-order Markov model can be obtained from [11]. Provided that the bits of an $M = 2^K$-ary symbol may be considered independent of each other, the channels' output information generated for the τth K-bit symbol is generated by the product of each of the constituent single-bit probabilities, which is given as

$$P[\hat{y}_\tau \,|\, y_\tau] = \prod_{k=1}^{K} P\left[\hat{y}_\tau(k) \,|\, y_\tau(k)\right] \tag{1}$$

where $\hat{y}_\tau = [\hat{y}_\tau(1), \hat{y}_\tau(2), \ldots, \hat{y}_\tau(K)]$ is the received K-bit SBC-coded sequence representing the τth M-ary, symbol, and $y_\tau = [y_\tau(1), y_\tau(2), \ldots, y_\tau(K)]$ is the corresponding transmitted bit sequence, again, provided that all these bits are independent of each other. For each desired bit $[y_\tau(\lambda)]$, extrinsic channel output information $P[\hat{y}_\tau^{[\mathrm{ext}]} \,|\, y_\tau^{[\mathrm{ext}]}]$ is expressed as

$$P\left[\hat{y}_\tau^{[\mathrm{ext}]} \,\middle|\, y_\tau^{[\mathrm{ext}]}\right] = \prod_{k=1, k\neq\lambda}^{K} P\left[\hat{y}_\tau(k) \,\middle|\, y_\tau(k)\right]. \tag{2}$$

Finally, the resultant extrinsic LLR value can be acquired for each bit of the τth symbol by combining its channel output information and the *a priori* knowledge of the corresponding τth symbol as [9], [11]

$$L\left[y_\tau(\lambda)\right] = \log\left(\frac{\sum_{y_\tau^{[\mathrm{ext}]}} P\left[y_\tau^{[\mathrm{ext}]} \,\middle|\, y_\tau(\lambda) = +1\right] \cdot P\left[\hat{y}_\tau^{[\mathrm{ext}]} \,\middle|\, y_\tau^{[\mathrm{ext}]}\right]}{\sum_{y_\tau^{[\mathrm{ext}]}} P\left[y_\tau^{[\mathrm{ext}]} \,\middle|\, y_\tau(\lambda) = -1\right] \cdot P\left[\hat{y}_\tau^{[\mathrm{ext}]} \,\middle|\, y_\tau^{[\mathrm{ext}]}\right]}\right). \tag{3}$$

Although the proposed technique is generic and, hence, is applicable to arbitrary speech, audio, and video source codecs, in our design example, the redundancy of the source-coded bit stream is characterized with the aid of the nonuniform M-ary symbol probability distribution[4] using the H.264/AVC video-encoded bit stream of the 300-frame "*Akiyo*" video sequence, the 150-frame "*Miss America*" video clip, and the 300-frame "*Mother&Daughter*" video sequence, which were used as training sequences.

III. SBC-Based Iterative Source Channel Decoding

A. Iterative Convergence

The purpose of ISCD is to utilize the constituent inner and outer decoders to assist each other in an iterative fashion to glean the highest possible extrinsic information [$L_{\mathrm{SBSD}}^{\mathrm{extr}}(x')$ and $L_{\mathrm{RSC}}^{\mathrm{extr}}(\bar{x})$] from each other. In fact, the achievable performance of SBSD is limited by the factor that its achievable iteration gain is actually dependent on the residual redundancy or correlation that remains in the coded bit pattern x_i after limited-complexity limited-delay lossy source encoding [1]. However, despite using limited-complexity limited-delay lossy compression, the achievable performance improvements of SBSD may remain limited due to the limited residual redundancy in the video-encoded bit stream when using the high-compression H.264/AVC video codec. It may be observed from the simulation results of [35] that typically using SBSD for the H.264/AVC-coded bit stream results in negligible system performance improvements beyond two decoding iterations. Hence, to improve the achievable ISCD performance gain, we *artificially* introduce redundancy in the source-coded bit stream using a technique that we refer to as SBC coding. The novel philosophy of our SBC design is based on exploiting a specific property of EXIT charts [36]. More explicitly, an iterative-decoding-aided receiver is capable of near-capacity operation at an infinitesimally low decoded bit error rate (BER), if there is an open tunnel between the EXIT curves of the inner and outer decoder components. We will demonstrate that this condition is clearly satisfied, when these two EXIT curves have a point of intersection at the $(I_A, I_B) = (1, 1)$ corner of the EXIT chart, where $I_A = I(x_i', L_{D,a})$, $0 \leq I_A \leq 1$ bit is the mutual information between the outer encoded bits x_i' and the LLR values $L_{D,a}$, whereas $I_E = I(x_i', L_{D,e})$, $0 \leq I_E \leq 1$ bit represents the mutual information between the outer channel-coded bits x_i' and the LLR values $L_{D,e}$. The *sufficient* and *necessary* condition for this iterative detection-convergence criterion to be met in the presence of perfect *a priori* information was shown in detail by Kliewer *et al.* [37] to be that the legitimate codewords have a minimum Hamming distance of $d_{\mathrm{H,min}} = 2$. Then, the ISCD scheme becomes capable of achieving the highest possible source entropy denoted as $H(X) = 1$ bit, provided that the input *a priori* information of the SBSD is perfect. This motivates the design of the proposed SBC schemes, because it is plausible that, using our design procedure, all legitimate SBC codewords having a specific mapping rate equivalent to the reciprocal of the classic code rate results in a code table satisfying the condition of $d_{\mathrm{H,min}} \geq 2$. Using appropriately

[3]The choice of how many bits are specifically grouped into an $M = 2^K$-ary symbol represents an important system parameter, but due to space limitations, this issue is not detailed in this paper.

[4]The resultant M-ary source word probability distribution for the $\mathrm{SBC}_{[K,N]}$ coding schemes used in our design example is not provided in this paper, owing to space limitations.

TABLE II
SBC CODING PROCEDURE USING ALGORITHM I

INPUT	OUTPUT COMBINATIONS			
Symbols	C_1	C_2	$\cdots$	C_{K+1}
$S_{(1)}$	$r_1 x_1 x_2 \cdots x_K$	$x_1 r_1 x_2 \cdots x_K$	.	$x_1 x_2 \cdots x_K r_1$
$S_{(2)}$	$r_2 x_1 x_2 \cdots x_K$	$x_1 r_2 x_2 \cdots x_K$	.	$x_1 x_2 \cdots x_K r_2$
$\vdots$	$\vdots$	$\vdots$	$\vdots$	$\vdots$
$S_{(2^K)}$	$r_{2^K} x_1 x_2 \cdots x_K$	$x_1 r_{2^K} x_2 \cdots x_K$	.	$x_1 x_2 \cdots x_K r_{2^K}$

TABLE III
SBC CODING PROCEDURE USING ALGORITHM II

INPUT	$x_1 x_2 \cdots x_K$				
STEPS	STEP-1				STEP-2
Repeated K-bit Concatenation	1^{st}	2^{nd}	$\cdots$	$(m+1)^{th}$	m^{th}
OUTPUT	$x_1 x_2 \cdots x_K$	$x_1 x_2 \cdots x_K$	$\cdots$	$x_1 x_2 \cdots x_K$	$x_1' x_2' \cdots x_K'$
	where, $x_1' = (0 \oplus x_2 \oplus \cdots x_K)$, $x_1' = (x_1 \oplus 0 \oplus \cdots x_K)$, $\cdots$ $x_K' = (x_1 \oplus x_2 \oplus \cdots 0)$				

designed SBCs, it may be guaranteed that the EXIT curve of the combined source codec and SBC block becomes capable of reaching the $(I_A, I_E) = (1, 1)$ point of perfect convergence, i.e., the maximum I_E will be taken at the $I_A = 1$ point of the EXIT chart [11], regardless of the EXIT curve shape of the standalone source encoder.

Having outlined the theoretical justification for achieving perfect convergence to an infinitesimally low BER, let us now introduce the proposed SBC$_{[K,N]}$ encoding algorithms, which map or encode each K-bit symbol of the source set X to the N-bit code words of the SBC set $f(X)$ while maintaining a minimum Hamming distance of $d_{\mathrm{H,min}} \geq 2$. According to our SBC$_{[K,N]}$ encoding procedure, video stream x_k is partitioned into $M = 2^K$-ary or K-bit source symbols, each of which has a different probability of occurrence and will alternatively be termed as the information word to be encoded into $N = (K + P)$ bits, where P represents the number of redundant bits per K-bit source symbol.

Algorithm I: For $P = 1$, the redundant bit r_τ is generated for the τth M-ary source symbol by calculating the exclusive-OR (XOR) function of its K constituent bits as follows:

$$r_\tau = [b^\tau(1) \quad \oplus \; b^\tau(2) \quad \cdots \quad \oplus \; b^\tau(K)] \tag{4}$$

where $\oplus$ represents the XOR operation.

The resultant redundant bit can be incorporated in any of the $[K + 1]$ different bit positions to create $[K + 1]$ different legitimate SBC-encoded words, as presented in Table II, each having a minimum Hamming distance of $d_{\mathrm{H,min}} = 2$ from all the others. The encoded symbols of the rate-2/3, -3/4, -4/5, and -5/6 SBCs, along with their corresponding minimum Hamming distance $d_{\mathrm{H,min}}$, is summarized in Table I for the specific case of incorporating the redundant bit r_τ at the end of the τth K-bit source symbol.

Algorithm II: For $P = (m \times K)$ with $m \geq 1$, we propose the corresponding SBC$_{[K,N]}$ encoding procedure, which results in a gradual increase in $d_{\mathrm{H,min}}$ for the coded symbols upon increasing both K and N of the SBC$_{[K,N]}$ while the code rate is fixed. This K-to-N-bit encoding method consists of two steps.

1) Step 1: $R_b = [(m-1) \times K]$ number of redundant bits $r_\tau(r)$, for $r = 1, 2, \ldots, R_b$, are concatenated to the τth K-bit source symbol by repeated concatenation of K additional source-coded bits $(m-1)$ times, yielding a total of $[(m-1) \times K]$ bits, as shown in Table III.
2) Step 2: The last set of K redundant bits $r_\tau(k)$, for $k = 1, 2, \ldots, K$, is generated by calculating the XOR function of the K source bits $b_\tau(j)$ while setting $b_\tau[j = k]$ equal to 0, yielding

$$r_\tau(k) = [b_\tau(1) \quad \oplus \; b_\tau(2) \quad \cdots \quad \oplus \; b_\tau(K)]$$

for $k = 1, 2, \ldots, K$, while setting $b_\tau(k) = 0$, as presented in Table III, where $\oplus$ represents the XOR operation.

Using this method, a carefully controlled redundancy is imposed by the specific rate $r = [K/N]$ SBC$_{[K,N]}$ to ensure that the resultant N-bit codewords exhibit a minimum Hamming distance of $d_{\mathrm{H,min}} \geq 2$ between the $M = 2^K$ number of legitimate K-bit source code words. This method also results in a gradual increase in the $d_{\mathrm{H,min}}$ of the coded symbols upon increasing both K and N of the SBC$_{[K,N]}$ considered, as shown in Table I, until the maximum achievable $d_{\mathrm{H,min}}$ is reached for the specific SBC coding rate.

B. Design Example

Let us now demonstrate the power of SBCs with the aid of a design example. As an example, the SBC$_{[K,N]}$-encoded symbols generated by applying rate-2/3, rate-3/4, rate-4/5, rate-5/6, and rate-1/3 coding schemes generated using Algorithms I and II are detailed in Table I, along with their corresponding minimum Hamming distances $d_{\mathrm{H,min}}$. Again, as it becomes evident from Table I, the EXIT-chart optimized SBCs ensure that the encoded N-bit symbols exhibit a minimum Hamming distance of $d_{\mathrm{H,min}} \geq 2$. Additionally, only 2^K out of the 2^N possible N-bit symbols are legitimate in the mapped source-coded bit stream, which exhibits a nonuniform probability of

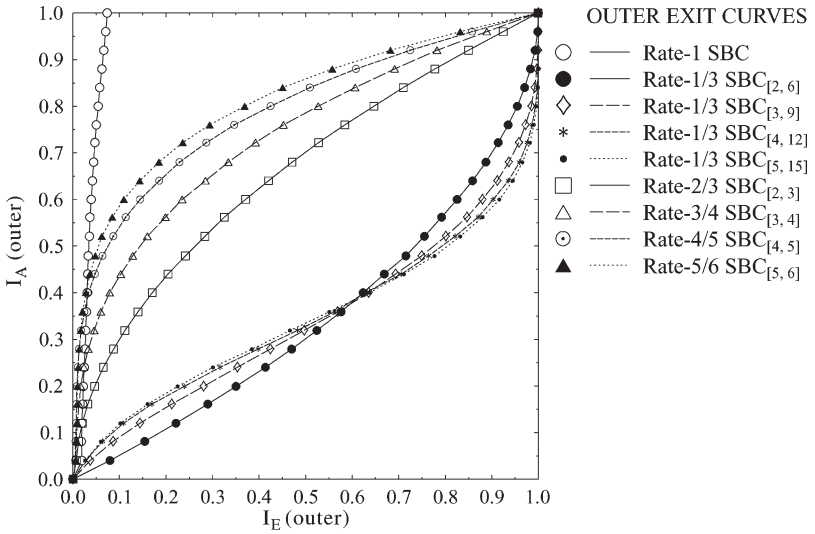

Fig. 2. EXIT characteristics of SBSD with the aid of different SBCs.

occurrence for the N-bit source symbols. Fig. 2 shows the EXIT characteristics of the SBSD scheme of Fig. 1 using either the rate-1[5] or the rate < 1 SBC$_{[K,N]}$ schemes of Algorithms I and II shown in Table I. More specifically, the EXIT curve of SBSD using rate-1/3, rate-2/3, rate-3/4, rate-4/5, and rate-5/6 SBCs does indeed reach to the top right corner of the EXIT chart at $(I_A, I_E) = (1, 1)$ and, hence, results in an infinitesimally low BER. By contrast, the SBSD scheme using a rate-1 SBC, i.e., no SBC, fails to do so. In conclusion, the simulation results recorded for the system presented in Fig. 1 reveal that the performance of SBSD strongly depends on the presence or absence of residual source redundancy, which typically manifests itself in the form of nonuniform probability of occurrence for the N-bit source-coded symbols. The coding parameters of the different SBC schemes used in our design example are shown in Table I. In this design example, our primary aim is to analyze the performance of the proposed *Algorithms I* and *II*, in conjunction with various SBCs having different coding rates and $d_{\mathrm{H,min}}$. For this reason, we selected rate-1/3 SBCs generated using *Algorithm II*, which provide sufficiently diverse $d_{\mathrm{H,min}}$ values of 3, 4, 5, and 6 to analyze the associated effects on the achievable performance while employing an RSC code as our inner code. Therefore, considering a rate-1/3 SBC code, along with a rate-3/4 inner RSC code, resulted in an overall system code rate of 1/4. We considered a concatenated RSC encoder with rate $R = 1/4$, constraint length $L = 4$, and generator sequences $g_1 = [1011]$, $g_2 = [1101]$, $g_3 = [1101]$, and $g_4 = [1111]$, which are represented as $G = [1, g2/g1, g3/g1, g4/g1]$; here, "1" denotes the systematic output; the first output g_1 is fed back to the input; and g_2, g_3, and g_4 denote the feedforward output of the RSC encoder. Additionally, for the SBC performance evaluation using our proposed system with a relatively high overall system code rate of $R = 1/2$ presented in Table I, we utilized a concatenated RSC encoder with rate $R = 1/2$, constraint length $L = 3$, and generator sequences $g_1 = [111]$ and $g_2 = [101]$, which are represented as $G = [1, g2/g1]$. Observe from the table that an overall code rate of $R = 1/4$ and $R = 1/2$ was maintained by adjusting the puncturing rate of the concatenated RSC to accommodate the different SBC rates of Table I.

[5]For the sake of using a unified terminology, we refer to the scheme using no SBC as the rate-1 SBC.

IV. Exit-Chart Analysis

At the receiver shown in Fig. 1, iterative soft-bit source and channel decoding is applied by exchanging extrinsic information between the receiver blocks, which has the capability of improving the achievable subjective video quality. EXIT charts were utilized to characterize the mutual information exchange between the input and output of both the inner and outer components of an iterative decoder and, hence, to analyze its decoding convergence behavior. Additionally, the actual decoding trajectories acquired while using various SBCs generated using Algorithms I and II were presented by recording the mutual information at the input and output of both the inner and outer decoders during the bit-by-bit Monte Carlo simulation of the iterative SBSD algorithm.

Fig. 3 shows the decoding trajectories recorded at $E_b/N_0 = 0$ and -1 dB, when employing the rate-2/3 SBCs of Algorithm I as the outer code, along with the corresponding rate-3/8 RSC code.

Furthermore, the decoding trajectories obtained by employing rate-1/3 outer SBCs of type SBC$_{[5,15]}$, which were generated using *Algorithm II*, and the rate-3/4 inner RSC detailed in Table I, were recorded at $E_b/N_0 = -4$ and -4.5 dB, as shown in Fig. 4. It may be observed from the EXIT trajectories of Figs. 3 and 4 that, as expected, the convergence behavior of the SBCs improves upon increasing $d_{\mathrm{H,min}}$.

V. System Performance Results

In this section, we present our performance results for the proposed system. A 45-frame "*Akiyo*" video sequence [1] in (176×144)-pixel quarter common intermediate format (QCIF) was used as our test sequence and was encoded using the H.264/AVC JM 13.2 reference video codec at 15 frames/s at the target bit rate of 64 kb/s. Using the H.264/AVC codec, each

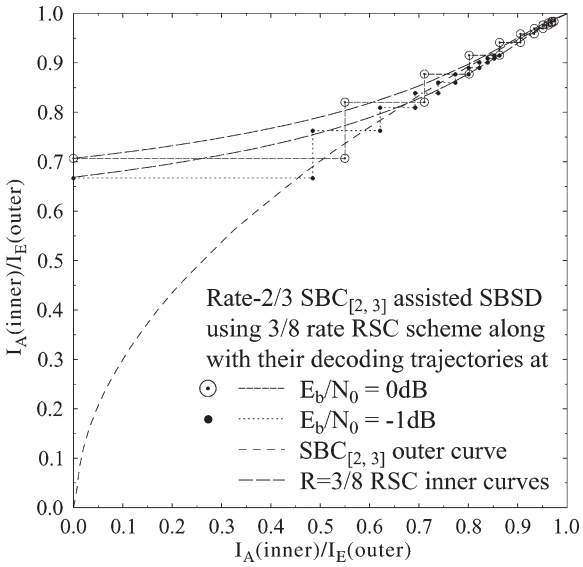

Fig. 3. EXIT chart and simulated decoding trajectories of the $\mathrm{SBC}_{[2,3]}$ scheme at $E_b/N_0 = 0$ and -1 dB.

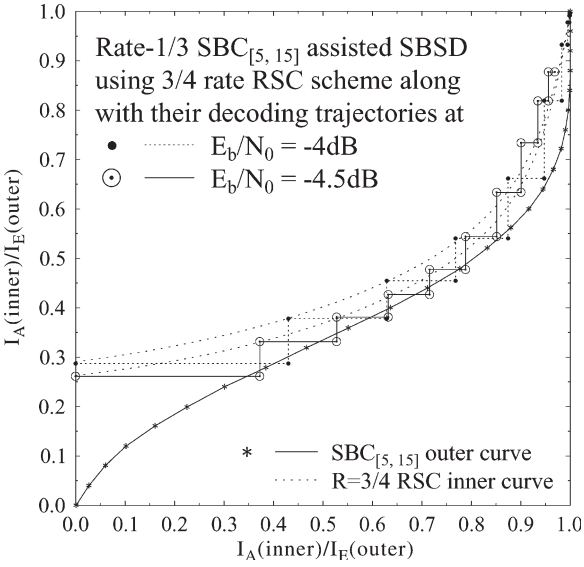

Fig. 4. EXIT chart and simulated decoding trajectories of the $\mathrm{SBC}_{[5,15]}$ scheme at $E_b/N_0 = -4$ and -4.5 dB.

QCIF frame was partitioned into nine slices, and each slice was composed of 11 MBs. The resultant video-encoded clip consisted of an intracoded "I" frame, followed by 44 predicted or "P" frames, corresponding to a lag of 3 s between the "I" frames at a frame rate of 15 frames/s. The periodic insertion of "I" frames curtailed error propagation beyond 45 frames.

Additional source codec parameters were set.

1) Quarter-pixel motion estimation resolution was used.
2) Intraframe MB update was used.
3) All MB types were enabled.
4) No multiframe prediction was used.
5) No B slices were used.
6) Universal-variable-length-coding-type entropy coding was used.
7) Error concealment was performed using the motion vector recovery algorithm of [38].

To control the effects of error propagation, we incorporated error resilience features, such as DP and intraframe-coded MB updates of three randomly distributed MBs per frame. The insertion of "B" pictures was avoided, because it results in an unacceptable loss of lip synchronization as a result of the corresponding delay incurred due to the bidirectionally predicted video-coding operations [38]. Additionally, only the immediately preceding frame was used for motion search, which results in reduced computational complexity, compared with that using multiple reference frames. These video-coding parameters were chosen, bearing in mind that the error resilience of the DP-aided H.264/AVC stream is directly related to the number of "P" frames inserted between two consecutive "I" frames.

The remaining error-resilient encoding techniques, such as the employment of multiple reference frames for interframe motion compensation and flexible MB ordering [39], were turned off because they typically result in modest video performance improvements in low-motion head-and-shoulders video sequences, such as the "*Akiyo*" clip, despite their substantially increased complexity. These encoder settings result in reduced encoder complexity and realistic real-time implementation. Moreover, since handheld videophones have to have low complexity, we limited the number of iterations between the RSC and SBSD decoders to $I_t = 10$, when using a rate-1 SBC, i.e., no SBC. Similarly, we used $I_t = 10$ iterations when applying SBCs having a rate below unity. For the sake of increasing the confidence in our results, we repeated each 45-frame experiment 160 times and averaged the results generated. A range of different SBCs generated using our proposed *Algorithms I* and *II* are given in Table I, which are used as the outer codes of Fig. 1 to evaluate their achievable system performance improvements. We evaluated the performance of our proposed system by keeping the same overall code rate and video rate for the different considered error protection schemes.

Fig. 5 shows the performance of the various rate-2/3, -3/4, -4/5, and -5/6 SBCs, along with the rate-1/3 SBC-based error protection schemes of Table I in terms of the attainable BER, in comparison with the rate-1 SBC-based scheme. Additionally, the performance trends expressed in terms of the peak SNR (PSNR) versus E_b/N_0 curves are shown in Fig. 6. It may be observed in Fig. 6 that the $\mathrm{SBC}_{[5,15]}$ scheme having $d_{\mathrm{H,min}} = 6$ provides the best PSNR performance among the eight different SBC schemes of Table I across the entire E_b/N_0 region considered. Furthermore, observe from Fig. 6 that the lowest rate-2/3 outer SBC, combined with rate-3/8 inner RSC, results in the best PSNR performance, outperforming the rate-3/4, rate-4/5, and rate-5/6 SBCs generated using Algorithm I. It may also be observed in Fig. 6 that using SBSD in conjunction with the rate-1 outer SBC and rate-1/4 inner RSC results in worse PSNR performance than the outer SBCs having a less-than-unity rate combined with the corresponding inner RSC of Table I while maintaining the same overall code rate. Additionally, Figs. 5 and 6 also present the BER and PSNR performance of our proposed system while employing rate-2/3 SBCs relative to the rate-1 SBC-based scheme, considering an overall system code rate of $R = 1/2$. Quantitatively, using the SBCs of Table I having a rate lower than 1 and overall system code rate of $R = 1/4$, an additional E_b/N_0 gain of up to 25 dB may be

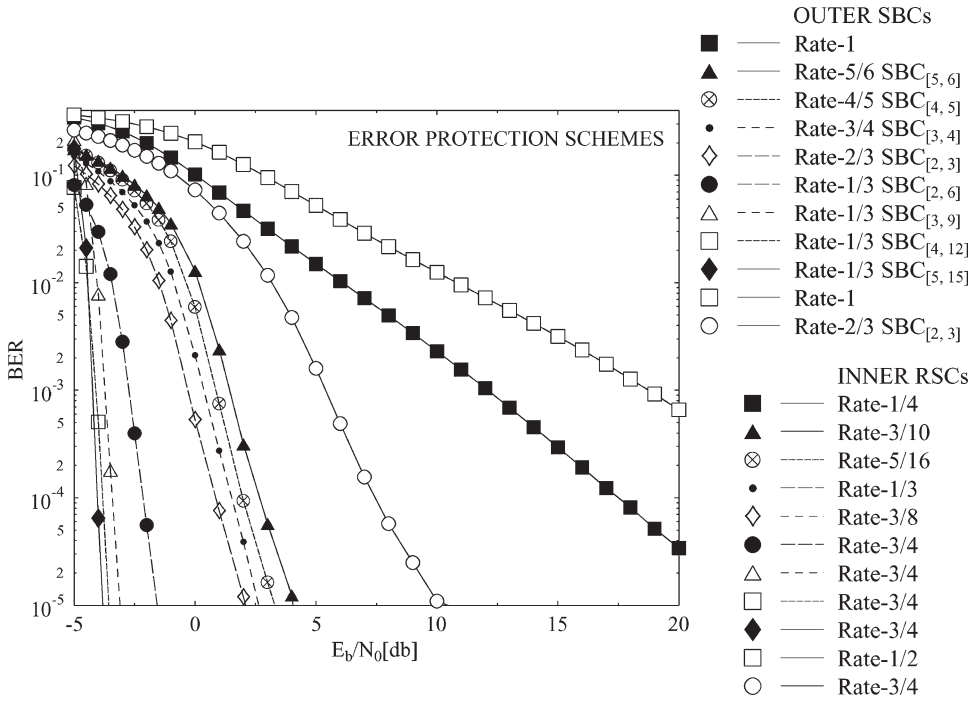

Fig. 5. BER versus E_b/N_0 performance of the various error protection schemes summarized in Table I.

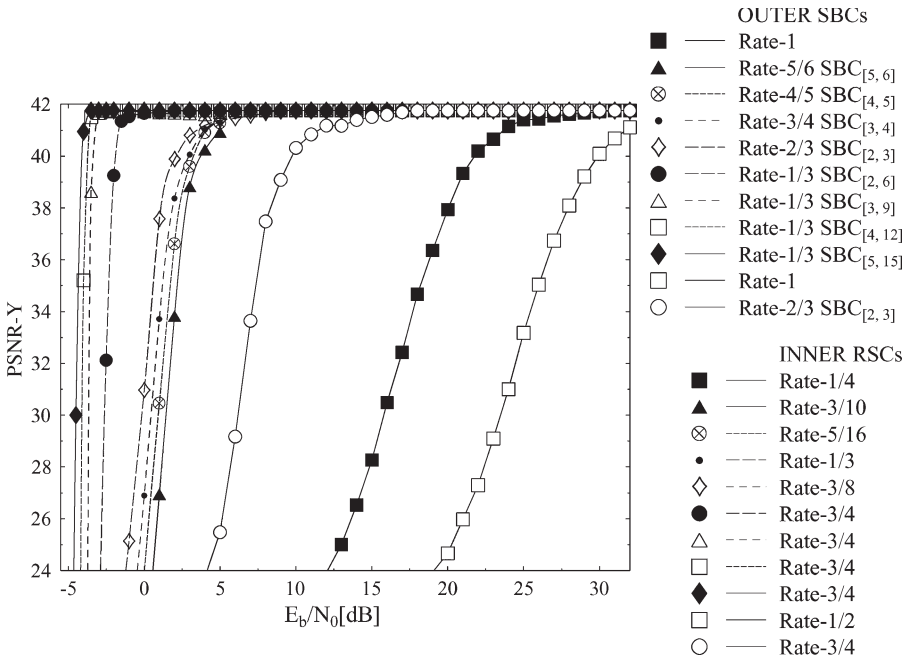

Fig. 6. PSNR-Y versus E_b/N_0 performance of various error protection schemes summarized in Table I.

achieved over the rate-1 SBC at the PSNR degradation point of 1 dB.

Finally, the achievable subjective video qualities of the video telephone schemes utilizing various types of SBCs generated using *Algorithms I* and *II* are presented in Figs. 7 and 8, respectively. To have a fair subjective video quality comparison, we averaged both the luminance and chrominance components of the 30 video test sequences, which were decoded using the H.264 video codec for each type of setup. The achievable subjective video quality recorded at the channel E_b/N_0 value of 0.5 dB using rate-2/3, rate-3/4, rate-4/5, and rate-5/6 SBCs of *Algorithm I* is shown in Fig. 7. Observe from Fig. 7 that the achievable video quality improves upon decreasing the SBC code rate.

Similarly, Fig. 8 shows the subjective video quality obtained at (left to right) $E_b/N_0 = -4.1$ dB, -3.9 dB, -3.0 dB, and -2.1 dB using rate-1/3 SBCs of type (top to bottom) $\text{SBC}_{[2,6]}$, $\text{SBC}_{[3,9]}$, $\text{SBC}_{[4,12]}$, and $\text{SBC}_{[5,15]}$. Observe from Fig. 8 that a nearly unimpaired quality is obtained for the rate-1/3 SBCs having (top to bottom) $d_{\text{H,min}} = 3, 4, 5,$ and 6 at E_b/N_0 values of -2.5, -3.0, -3.9, and -4.1 dB, respectively. This implies that the subjective video quality of the system improves upon increasing $d_{\text{H,min}}$ of the SBCs employed.

Fig. 7. Subjective video quality of the 45th "*Akiyo*" video sequence frame using (left to right) rate-2/3, rate-3/4, rate-4/5, and rate-5/6 SBCs of Algorithm I summarized in Table I at $E_b/N_0 = 0.5$ dB.

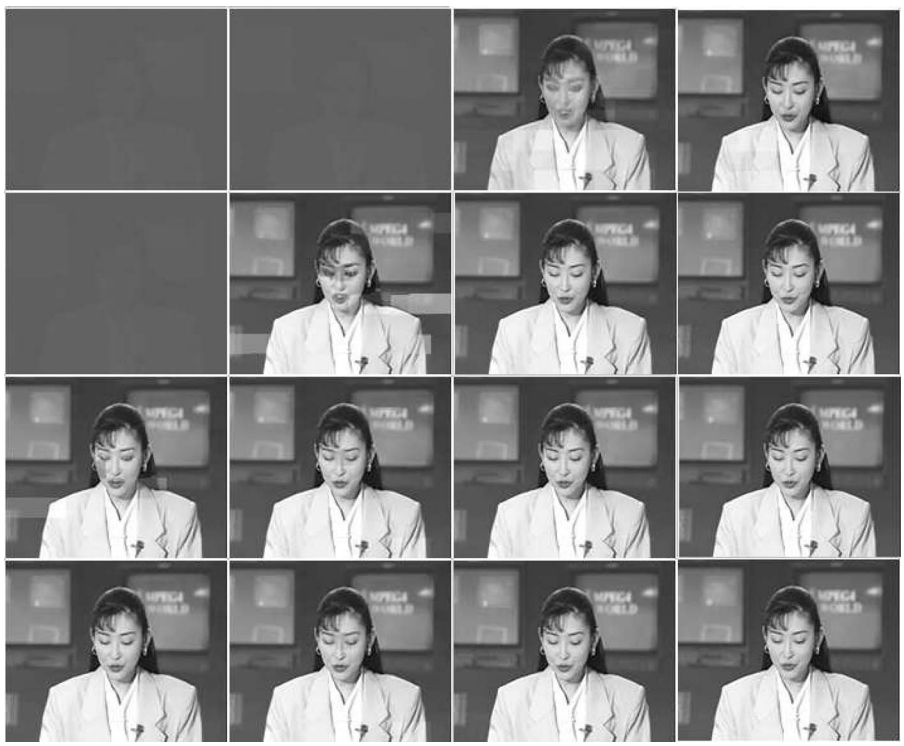

Fig. 8. Subjective video quality of the forty-fifth "*Akiyo*" video sequence frame using rate-1/3 SBCs of type (top to bottom) $\mathrm{SBC}_{[2,6]}$, $\mathrm{SBC}_{[3,9]}$, $\mathrm{SBC}_{[4,12]}$, and $\mathrm{SBC}_{[5,15]}$ of Algorithm II summarized in Table I at (left to right) $E_b/N_0 = -4.1$ dB, -3.9 dB, -3 dB, and -2.1 dB.

VI. Conclusion

In this paper, we have proposed generic low-complexity SBCs for satisfying the *necessary* and *sufficient* condition of $d_{\mathrm{H,min}} = 2$, hence guaranteeing decoding convergence for arbitrary SBSD-aided multimedia source codecs. We have applied diverse error-protection schemes considering the transmission of DP-aided H.264/AVC-coded video using carefully selected SBCs having diverse $d_{\mathrm{H,min}}$ values. Furthermore, iterative soft-bit source and channel decoding has been used to enhance the attainable BER performance and improve the objective video quality expressed in terms of PSNR. It has been demonstrated that the bit-error correction capability of the ISCD scheme was significantly improved with the advent of the rate-1/3 SBC scheme, owing to the intentional increase in redundancy of the source-coded bit stream, when we beneficially partitioned the total available bit rate budget between the source and channel codecs. Additionally, the convergence behavior of the ISCD system has been analyzed using EXIT charts. The H.264/SBC/RSC design example using SBCs having $d_{\mathrm{H,min}} = 6$ has exhibited an E_b/N_0 gain of 2.25 dB at the PSNR degradation point of 1 dB over the identical-rate SBCs having $d_{\mathrm{H,min}} = 3$. Additionally, an E_b/N_0 gain of 9 dB has been achieved, compared with the rate-5/6 SBCs having $d_{\mathrm{H,min}} = 2$ and an identical overall code rate. Moreover, an E_b/N_0 gain of 25 dB has been attained at the PSNR degradation point of 1 dB using iterative soft-bit source and channel decoding with the aid of rate-1/3 SBCs, in comparison with the identical-rate benchmarker. Our future research will consider the design of systematic variable-length SBC coding techniques to intentionally introduce redundancy in the source-coded bit stream based on the relative importance of the different H.264/AVC partitions.

References

[1] L. Hanzo, P. Cherriman, and J. Streit, *Video Compression and Communications: From Basics to H.261, H.263, H.264, MPEG2, MPEG4 for DVB and HSDPA-Style Adaptive Turbo-Transceivers*. New York: Wiley, 2007.

[2] L. Hanzo, C. Somerville, and J. Woodard, *Voice and Audio Compression for Wireless Communications*, 2nd ed. New York: Wiley, 2007.

[3] R. Stedman, H. Gharavi, L. Hanzo, and R. Steele, "Transmission of subband-coded images via mobile channels," *IEEE Trans. Circuits Syst. Video Technol.*, vol. 3, no. 1, pp. 15–26, Feb. 1993.

[4] L. Hanzo and J. Streit, "Adaptive low-rate wireless videophone schemes," *IEEE Trans. Circuits Syst. Video Technol.*, vol. 5, no. 4, pp. 305–318, Aug. 1995.

[5] J. Streit and L. Hanzo, "Dual-mode vector-quantized low-rate cordless videophone systems for indoors and outdoors applications," *IEEE Trans. Veh. Technol.*, vol. 46, no. 2, pp. 340–357, May 1997.
[6] J. Streit and L. Hanzo, "Quadtree-based reconfigurable cordless videophone systems," *IEEE Trans. Circuits Syst. Video Technol.*, vol. 6, no. 2, pp. 225–237, Apr. 1996.
[7] L. Hanzo, P. Cherriman, and E. L. Kuan, "Interactive cellular and cordless video telephony: State-of-the-art system design principles and expected performance," *Proc. IEEE*, vol. 88, no. 9, pp. 1388–1413, Sep. 2000.
[8] S. X. Ng, J. Y. Chung, and L. Hanzo, "Turbo-detected unequal protection MPEG-4 wireless video telephony using multi-level coding, trellis coded modulation and space-time trellis coding," *Proc. Inst. Elect. Eng.—Commun.*, vol. 152, no. 6, pp. 1116–1124, Dec. 2005.
[9] T. Fingscheidt and P. Vary, "Softbit speech decoding: A new approach to error concealment," *IEEE Trans. Speech Audio Process.*, vol. 9, no. 3, pp. 240–251, Mar. 2001.
[10] T. Fingscheidt, S. Heinen, and P. Vary, "Joint speech codec parameter and channel decoding of parameter individual block codes (PIBC)," in *Proc. IEEE Workshop Speech Coding*, Porvoo, Finland, 1999, pp. 75–77.
[11] M. Adrat and P. Vary, "Iterative source-channel decoding: Improved system design using exit charts," *EURASIP J. Appl. Signal Process.*, vol. 2005, no. 1, pp. 928–941, Jan. 2005.
[12] R. Perkert, M. Kaindl, and T. Hindelang, "Iterative source and channel decoding for GSM," in *Proc. IEEE ICASSP*, Salt Lake City, UT, 2001, vol. 4, pp. 2649–2652.
[13] J. Ostermann, J. Bormans, P. List, D. Marpe, M. Narroschke, F. Pereira, T. Stockhammer, and T. Wedi, "Video coding with H.264/AVC: Tools, performance, and complexity," *IEEE Circuits Syst. Mag.*, vol. 4, no. 1, pp. 7–28, May 2004.
[14] A. Guyader, E. Fabre, C. Guillemot, and M. Robert, "Joint source-channel turbo decoding of entropy-coded sources," *IEEE J. Sel. Areas Commun.*, vol. 19, no. 9, pp. 1680–1696, Sep. 2001.
[15] J. Kliewer and R. Thobaben, "Iterative joint source-channel decoding of variable-length codes using residual source redundancy," *IEEE Trans. Wireless Commun.*, vol. 4, no. 3, pp. 919–929, May 2005.
[16] J. Liu, G. Tu, C. Zhang, and Y. Yang, "Joint source and channel decoding for variable length encoded turbo codes," *EURASIP J. Adv. Signal Process.*, vol. 2008, no. 1, pp. 1–10, Jan. 2008.
[17] R. G. Maunder, J. Wang, S. X. Ng, L. L. Yang, and L. Hanzo, "On the performance and complexity of irregular variable length codes for near-capacity joint source and channel coding," *IEEE Trans. Wireless Commun.*, vol. 7, no. 4, pp. 1338–1347, Apr. 2008.
[18] L. Hanzo, J. Blogh, and S. Ni, *3G, HSPA and FDD versus TDD Networking: Smart Antennas and Adaptive Modulation*, 2nd ed. New York: Wiley, Feb. 2008.
[19] L. Hanzo, T. H. Liew, and B. L. Yeap, *Turbo Coding, Turbo Equalization and Space-Time Coding for Transmission Over Fading Channels*. New York: Wiley, 2002.
[20] A. Q. Pham, J. Wang, L. L. Yang, and L. Hanzo, "An iterative detection aided irregular convolutional coded wavelet videophone scheme using reversible variable-length codes and map equalization," in *Proc. IEEE 65th VTC—Spring*, Dublin, Ireland, Apr. 2007, pp. 2404–2408.
[21] Nasruminallah, M. El-Hajjar, N. Othman, A. Quang, and L. Hanzo, "Over-complete mapping aided, soft-bit assisted iterative unequal error protection H.264 joint source and channel decoding," in *Proc. IEEE VTC—Fall*, Sep. 2008, pp. 1–5.
[22] Y. Wang and S. Yu, "Joint source-channel decoding for H.264 coded video stream," *IEEE Trans. Consum. Electron.*, vol. 51, no. 4, pp. 1273–1276, Nov. 2005.
[23] T. Clevorn, P. Vary, and M. Adrat, "Iterative source-channel decoding using short block codes," in *Proc. ICASSP*, May 2006, vol. 4, p. IV.
[24] R. Thobaben, "A new transmitter concept for iteratively-decoded source-channel coding schemes," in *IEEE 8th Workshop SPAWC*, Jun. 2007, pp. 1–5.
[25] R. Thobaben, L. Schmalen, and P. Vary, "Joint source-channel coding with inner irregular codes," in *Proc. IEEE ISIT*, Jul. 2008, pp. 1153–1157.
[26] M. Adrat, P. Vary, and T. Clevorn, "Optimized bit rate allocation for iterative source-channel decoding and its extension towards multi-mode transmission," in *Proc. IST Mobile Wireless Commun. Summit*, Dresden, Germany, Jun. 2005, pp. 1153–1157.
[27] T. Clevorn, J. Brauers, M. Adrat, and P. Vary, "Turbo decodulation: Iterative combined demodulation and source-channel decoding," *IEEE Commun. Lett.*, vol. 9, no. 9, pp. 820–822, Sep. 2005.
[28] T. Clevorn, J. Braucrs, M. Adrat, and P. Vary, "EXIT chart analysis of turbo decodulation," in *Proc. IEEE 16th Int. Symp. PIMRC*, Sep. 2005, vol. 2, pp. 711–715.
[29] T. Clevorn, M. Adrat, and P. Vary, "Turbo decodulation using highly redundant index assignments and multi-dimensional mappings," in *Proc. Int. Symp. Turbo Codes Related Topics*, Munich, Germany, Apr. 2006.
[30] T. Clevorn, L. Schmalen, P. Vary, and M. Adrat, "On redundant index assignments for iterative source-channel decoding," *IEEE Commun. Lett.*, vol. 12, no. 7, pp. 514–516, Jul. 2008.
[31] T. Wiegand, G. J. Sullivan, G. Bjntegaard, and A. Luthra, "Overview of the H.264/AVC video coding standard," *IEEE Trans. Circuits Syst. Video Technol.*, vol. 13, no. 7, pp. 560–576, Jul. 2003.
[32] *H.264: Advanced Video Coding for Generic Audiovisual Services*, p. 282, May 2003. ITU-T: H.264 Recommendation. [Online]. Available: www.itu.int/rec/T-REC-H.264/en
[33] R. G. Maunder, J. Kliewer, S. X. Ng, J. Wang, L. L. Yang, and L. Hanzo, "Joint iterative decoding of trellis-based VQ and TCM," *IEEE Trans. Wireless Commun.*, vol. 6, no. 4, pp. 1327–1336, Apr. 2007.
[34] S. Benedetto, D. Divsalar, G. Montorsi, and F. Pollara, "Serial concatenation of interleaved codes: Performance analysis, design and iterative decoding," *IEEE Trans. Inf. Theory*, vol. 44, no. 3, pp. 909–926, May 1998.
[35] T. Hindelang, M. Adrat, T. Fingscheidt, and S. Heinen, "Joint source and channel coding: From the beginning until the 'EXIT,"' *Eur. Trans. Telecommun.*, vol. 18, no. 8, pp. 851–858, 2007.
[36] S. ten Brink, "Designing iterative decoding schemes with the extrinsic information transfer chart," *AEU Int. J. Electron. Commun.*, vol. 54, pp. 389–398, Nov. 2000.
[37] J. Kliewer, N. Goertz, and A. Mertins, "Iterative source-channel decoding with Markov random field source models," *IEEE Trans. Signal Process.*, vol. 54, no. 10, pp. 3688–3701, Oct. 2006.
[38] T. Stockhammer, M. M. Hannuksela, and T. Wiegand, "H.264/AVC in wireless environments," *IEEE Trans. Circuits Syst. Video Technol.*, vol. 13, no. 7, pp. 657–673, Jul. 2003.
[39] S. Wenger, "H.264/AVC over IP," *IEEE Trans. Circuits Syst. Video Technol.*, vol. 13, no. 7, pp. 645–656, Jul. 2003.

Nasruminallah received the B.Sc. degree in computer engineering from the University of Engineering and Technology, Peshawar, Pakistan, in 2004 and the M.Sc. degree in computer engineering from Lahore University of Management Sciences, Lahore, Pakistan, in 2006. He is currently working toward the Ph.D. degree with the Communications Group, School of Electronics and Computer Science, University of Southampton, Southampton, U.K.

His research interests include low-bit-rate video coding for wireless communications, turbo coding and detection, and iterative source-channel decoding.

Lajos Hanzo (M'91–SM'92–F'04) received the M.S. degree in electronics and the Ph.D. degree from Technical University of Budapest, Budapest, Hungary, in 1976 and 1983, respectively, and the D.Sc. degree from the University of Southampton, Southampton, U.K., in 2004.

During his career in telecommunications, he has held various research and academic posts in Hungary, Germany, and the U.K. Since 1986, he has been with the Department of Electronics and Computer Science, University of Southampton, where he holds the Chair in telecommunications. He currently heads an academic research team, working on a range of research projects in the field of wireless multimedia communications sponsored by the industry, the Engineering and Physical Sciences Research Council U.K., the European IST Program, and the Mobile Virtual Centre of Excellence, U.K. He is an enthusiastic supporter of industrial and academic liaison and offers a range of industrial courses. He has coauthored 15 John Wiley and IEEE Press books, totaling to 10 000 pages on mobile radio communications, has published about 700 research papers, organized and chaired conferences, and presented various keynote and overview lectures.

Dr. Hanzo is a Fellow of the Royal Academy of Engineering and the Institution of Electrical Engineers. He is an IEEE Distinguished Lecturer of the Communications and Vehicular Technology (VT) Societies. He serves on the Editorial Board of the PROCEEDINGS OF THE IEEE and is a Governor of the IEEE VT Society. He has been the recipient of a number of distinctions.